2007

Demonstration of Magnetoelectric Scanning Probe Microscopy

Jason R. Hattrick-Simpers
University of South Carolina - Columbia, simpers@cec.sc.edu

Liyang Dai

Manfred Wuttig

Ichiro Takeuchi

Eckhard Quandt

Publication Info

Published in *Review of Scientific Instruments*, Volume 78, Issue 10, 2007, pages #106103-.

Hattrick-Simpers, J. R., Dai, L., Wutting, M., Takeuchi, I., & Quandt, E. (October 2007). Demonstration of Magnetoelectric Scanning Probe Microscopy. Review of Scientific Instruments, 78 (10), #106103.
http://dx.doi.org/10.1063/1.2777197

AIP | Review of Scientific Instruments

Demonstration of magnetoelectric scanning probe microscopy

Jason R. Hattrick-Simpers, Liyang Dai, Manfred Wuttig, Ichiro Takeuchi, and Eckhard Quandt

Citation: Review of Scientific Instruments **78**, 106103 (2007); doi: 10.1063/1.2777197
View online: http://dx.doi.org/10.1063/1.2777197
View Table of Contents: http://scitation.aip.org/content/aip/journal/rsi/78/10?ver=pdfcov
Published by the AIP Publishing

Demonstration of magnetoelectric scanning probe microscopy

Jason R. Hattrick-Simpers, Liyang Dai, Manfred Wuttig, and Ichiro Takeuchi[a)]
Department of Materials Science and Engineering, University of Maryland, College Park, Maryland 20742

Eckhard Quandt
Caesar, Bonn 53175, Germany

(Received 16 January 2007; accepted 6 August 2007; published online 4 October 2007)

A near-field room temperature scanning magnetic probe microscope has been developed using a laminated magnetoelectric sensor. The simple trilayer longitudinal-transverse mode sensor, fabricated using Metglas as the magnetostrictive layer and polyvinylidene fluoride as the piezoelectric layer, shows an ac field sensitivity of 467 ± 3 μV/Oe in the measured frequency range of 200 Hz–8 kHz. The microscope was used to image a 2 mm diameter ring carrying an ac current as low as 10^{-5} A. ac fields as small as 3×10^{-10} T have been detected. © *2007 American Institute of Physics.* [DOI: 10.1063/1.2777197]

Scanning magnetic probe microscopes using high sensitivity magnetometers are vital for applications ranging from nondestructive evaluation of integrated circuits to the investigation of magnetic materials. Common to scanning magnetic probe microscopes is the trade off between spatial resolution, sensitivity, and operating conditions. Magnetic force microscopy (MFM), for instance, has spatial resolution as high as 10 nm at room temperature.[1,2] However, it measures field gradients instead of actual fields, and its typical reported field sensitivity is 10^{-4} T.[2] Recently, scanning Hall probe microscopes have shown spatial resolutions as high as 50 nm with field sensitivities down to 10^{-8} T.[2,3] Superconducting quantum interference devices (SQUIDs) are known to be the highest sensitivity magnetometers, capable of detecting single flux quanta, and have been incorporated in scanning microscopes. For low temperature scanning SQUID microscopes using Nb-based SQUIDs, the maximum demonstrated field sensitivity is 2×10^{-14} T/Hz$^{1/2}$.[4] The spatial resolution of this type of scanning SQUID is limited only by the size of the device, but measurements must be carried out with the sample at cryogenic temperatures.[4] In room temperature scanning SQUID microscopes, a sapphire window is placed between the cryogenically cooled SQUID sensor and the room temperature sample. The best demonstrated sensitivity for these systems is 10^{-14} T/Hz$^{1/2}$.[2] However, the distance between the sample and the sensor limits the spatial resolution to 20 μm.[2,4] Recently, tunneling magnetoresistance sensors have been incorporated in probe microscopes with spatial resolutions as high as 0.1 μm and a demonstrated field sensitivity of 10^{-9} T.[5]

Magnetoelectric (ME) materials are material systems that simultaneously display ferromagnetism and ferroelectricity. Laminated magnetoelectrics, a subclass of magnetoelectric materials, have gained significant attention in the past few years due to their ability to sense very small magnetic fields.[6–10] The laminates are created by bonding magnetostrictive and piezoelectric materials into layered structures that are elastically coupled. When the laminate is exposed to a magnetic field, the stress caused by the magnetostrictive material is transferred to the piezoelectric layer. This causes a strain in the piezoelectric resulting in a voltage. Laminated magnetoelectric structures have been used to demonstrate ac field sensitivity as high as 10^{-15} T/Hz$^{1/2}$ at room temperature when operated at the mechanical resonance ($\sim10^5$ Hz) of the sensor.[10] These devices are inexpensive to manufacture and operate at room temperature. Such properties make ME sensors attractive for scanning magnetic probe applications.

Here, we report on the fabrication of a prototype near-field scanning magnetic probe using a ME device, fabricated from high magnetic permeability Metglas and polyvinylidene fluoride (PVDF). The use of Metglas ensures that the required dc biasing magnetic field remains low, without sacrificing the ME sensitivity. Through calibration of the device prior to use, it is shown that the laminated sensors can obtain spatially resolved mappings of minute ac magnetic fields. Scans across a 2 mm diameter current bearing ring have illustrated the feasibility of using such devices as scanning magnetic probes, where the spatial resolution is primarily limited by the device dimensions.

ME materials incorporating high magnetic permeability materials can show large ME elastic coupling; the ME response of a laminate is directly related to its magnetic permeability. The strength of the ME coupling is given by the ME coefficient $\alpha^E=\partial E/\partial H$, which expresses the induced electric field (E) due to a change in magnetic field (H). Because the electric field here is the transduced piezovoltage, α^E can be rewritten in terms of the magnetostrictive susceptibility,

$$\frac{\partial E}{\partial H}=\frac{\partial E}{\partial \varepsilon}\frac{\partial \varepsilon}{\partial H}=\frac{\partial E}{\partial \varepsilon}\frac{\partial \lambda}{\partial H}, \tag{1}$$

where ε is the transduced strain and is equal to the magnetostriction (λ) assuming ideal coupling between the magnetostrictive and piezoelectric layers. The magnetostrictive permeability $\partial\lambda/\partial H$ of a material is, in turn, related to its magnetic permeability χ_m,

[a)]Also at Center for Superconductivity Research, University of Maryland, College Park, MD 20742. Electronic mail: takeuchi@umd.edu

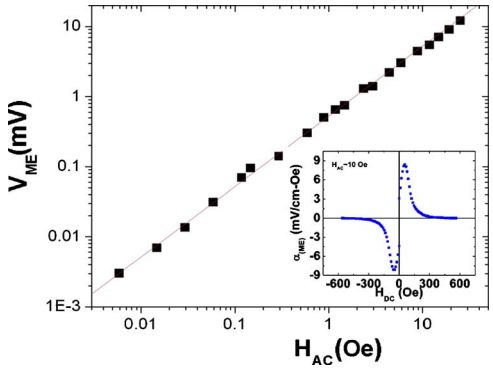

FIG. 1. (Color online) ME signal vs ac field. The slope of the curve indicates that the sensor has a sensitivity of 467 μV/Oe over an ac field range of 10^{-6}–10^{3} T. The inset shows a calibration scan of a ME device. The peak in ME signal is 8.6±.1 mV/(cm Oe) at an applied dc field of 70 Oe with an H_{ac} of 10 Oe.

$$\frac{\partial \lambda}{\partial H} = \frac{\partial \lambda}{\partial M}\frac{\partial M}{\partial H} = \frac{\partial \lambda}{\partial M}\chi_m. \tag{2}$$

Thus, one can maximize α^E by biasing the device at a field where $\partial M/\partial H = \chi_m$ is maximum. This makes ME devices incorporating high permeability magnetic materials attractive as high response ME devices. The required dc bias for peak performance is significantly lower than in devices using lower χ_m materials such as $Fe_{80}Ga_{20}$ and $Fe_2Tb_{.3}Dy_{.7}$. From an applications perspective this is very desirable.

The ME sensor was fabricated using commercially available Metglas and PVDF samples. Metglas was chosen as the magnetostrictive material, despite its low magnetostriction, because it exhibits a relative permeability as high as 400 000 at a field of less than 1 Oe. This permeability is a factor of 40 000 greater than the permeablility of $Fe_2Tb_{.3}Dy_{.7}$, which is known to exhibit the highest magnetostriction of all magnetostrictors.[11] We used a 23 μm thick Metglas foil, which was field annealed to give a saturation magnetostriction of 30 ppm along the rolling direction of the ribbon. It was cut in 4×2 mm^2 pieces with the field annealing direction parallel to the long dimension. PVDF was chosen for its high piezoelectric response as well as its superior deformability compared to traditional oxide ferroelectrics. A 100 μm thick sheet of PVDF was cut into 6×6 mm^2 and was electrically poled perpendicular to the plane of the film. The Metglas and the PVDF were bonded into a trilayer laminated structure with a conductive epoxy. This configuration has a longitudinal-transverse ME laminate structure. The active device dimensions are 2 mm$\times$4 mm$\times$146 μm.

The sensors were calibrated for their ac and dc magnetic field responses prior to their use in the scanning probe. The dc field dependence was measured for a series of constant ac bias fields to determine the peak dc bias field. Both fields were applied along the field annealing direction of the Metglas. The ac field response of the sensor was tested in the frequency range of 200 Hz$<f<$8 kHz for ac amplitudes from 20 to 10^{-5} Oe. The ME signal was found to be independent of frequency in the range studied here thereby indicating that no inductive voltage signal was detected. Figure 1 shows a summary of the peak ME response as a function of ac field amplitude at 259 Hz. The ac sensitivity of the sensor, taken as the slope of the line from Fig. 1, is 467±3 μV/Oe.

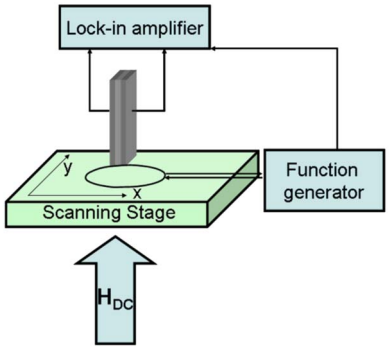

FIG. 2. (Color online) A schematic of the scanning near-field magnetic field probe setup. The dc field is applied parallel to the field annealed axis of the Metglas. A motion control program is used to scan the sensor across the ring. The active part of the trilayer device is shown.

The inset of figure shows a representative ME signal versus applied dc magnetic field plot at an ac magnetic field amplitude of 10 Oe. The ME signal has a maximum of 8.6±.1 mV/(cm Oe) at a dc bias field of 70 Oe.

Although the intrinsic coercive field of the Metglas sheet is less than 1 Oe, the peak in ME signal is seen at 70 Oe. The increase in coercivity is likely a consequence of the substantial demagnetizing field due to the sensor geometry.[12]

To demonstrate the utility of the ME device as a scanning probe microscope, the ME device was mounted onto a scanning stage and scanned across a ring carrying an ac current. The 2 mm diameter current carrying ring was made from a 50 gauge Cu wire. A constant dc magnetic field of 70 Oe was applied parallel to the field annealed axis of the device with a Helmholtz coil. Figure 2 shows the schematic of the experiment and orientation of the sensor with respect to the current carrying ring. The field annealed axis of the sensor was placed perpendicularly to the plane of the ring. This was to ensure the sensor would be sensitive predominantly to the out-of-plane component of the magnetic field H_z.

Figure 3 is a line scan taken while the sensor was scanned along its thickness direction through the center of the ring (x direction in Fig. 2). During scanning the sensor was maintained at a distance of 50 μm from the plane of the ring, while the ME signal was recorded every 150 μm. The ac current through the ring was fixed at 150 mA at a fre-

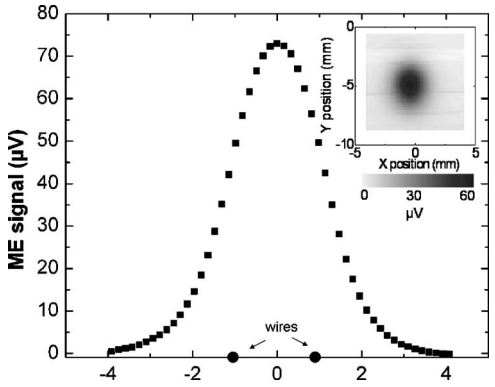

FIG. 3. A one-dimensional (1D) scan of a ring carrying a current of 150 mA. The cross section of the wires of the ring is shown to denote the wire position, but is not to scale.

quency of 5 kHz. The position of the ring wire cross sections relative to the signal is denoted in the figure by the black circles.

Looking closely at the line scan from Fig. 3, and taking into consideration the dimensions of our device (146 μm$\times$2 mm$\times$4 mm) and a scanning height of 50 μm, the measured magnetic field displays a broadened profile. The discrepancy results from the fact that (1) in any near-field scanning device the spatial resolution is comparable to the device dimension, and (2) the magnetic permeability of the Metglas is distorting the magnetic field distribution of the ring over the dimensions of the device.

A finite element analysis, using the software FEMM™, was performed (not shown here) to confirm that the presence of the Metglas alters the field distribution of a current carrying wire, and that the extent to which the field redistribution takes place is of the order of the device size. To examine the possible effect of the extremely high permeability of Metglas, calculations were performed for materials with μ=400 000 as well as μ=40. We found that the degree to which the field redistribution takes place and the length scale over which it occurs were comparable in both cases.

The local field distortion present in near-field scanning magnetic probe techniques using magnetic sensors is known. For instance, in MFM, the interaction between the magnetic tip and sample surface is known to affect the local field distribution. To accurately and precisely interpret the images, significant postmeasurement deconvolution involving detailed knowledge of tip geometry and magnetic properties is required.[13,14] The active sensing area that needs to be modeled for deconvolution in MFM studies is of the order of the tip dimensions. Similarly, in the present magnetic trilayer device, field redistribution is expected for dimensions comparable to the device size.

The inset of Fig. 3 shows a two-dimensional (2D) scan taken over the same ring with the same condition as the line scan. The distortion of the overall shape of the ring "image" to an oval one is due to the disparity in the dimensions of the sensor in the plane of the ring, 146 μm through the thickness (x direction) and 2 mm across the width (y direction), as well as the redistribution of the field lines. This implies that decreasing the size of the device can contribute to improving the spatial resolution.

In order to establish the lowest field detectable using the current sensors, a series of line scans were taken, at a constant frequency of 5 kHz, with decreasing ac currents. The results from these scans are shown in Fig. 4, where the results from the three lowest currents are displayed. From these data, it is clear that for 150 μA, the peak in the signal from the ring is still clearly evident. From the Bio-Savart law, 1 mm away from the edge of the ring, the field possesses only a vertical component. The field experienced by the sensor at this point is calculated to be 1.5×10^{-10} T. This calculated value is of the same order of magnitude as the value calculated using the slope of the ac sensitivity from Fig. 1, and we take this to be the minimum detectable field with the current sensor. This corresponds to a maximum sensitivity of 3×10^{-10} T. Using the measurement bandwidth of 0.33 Hz, the sensitivity of the present sensor is $\approx5\times10^{-10}$ T/Hz$^{1/2}$.

We have demonstrated that simple bonded Metglas/PVDF trilayer devices can be used to make a near-field scanning magnetic field probe with a sensitivity of 10^{-10} T and a spatial resolution roughly determined by the device size. It is of interest from an application's point of view to increase the spatial resolution by orders of magnitude. We have found, however, that our present method of laminate bonding precludes us from pursuing smaller device dimensions as there is inhomogeneity in the bonding of the trilayer. The length scale of this inhomogeniety is of the order of hundreds of microns and precludes reducing the device size down to less than 1 mm. Alternative methods of fabricating devices and, in particular, bonding techniques are currently being pursued so that we can work toward reducing the device size, and hence the spatial resolution of the scanning magnetic probe.

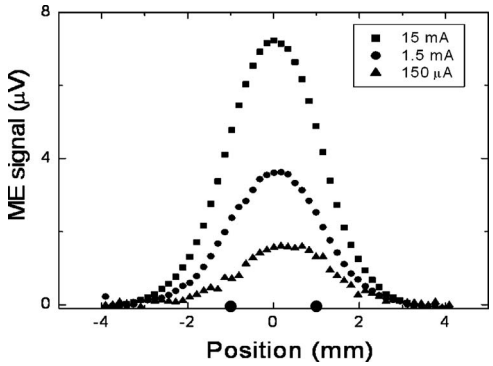

FIG. 4. A series of line scans taken for different I_{ac} through the ring. The data have been multiplied by 1, 5, and 30 for 15 mA, 1.5 mA, and 150 μA, respectively. The cross section of the wires of the ring is shown to denote the wire position, but is not to scale.

The authors gratefully acknowledge valuable discussions with Samuel E. Lofland. This work was supported by ONR-MURI Grant Nos. N000140110761, N000140610530, and NSF-MRSEC DMR 0520471 as well as NSF-DMR Grant No. 0354740. This work was also supported in part by the IMI Program of the National Science Foundation under Award No. DMR-0603644.

[1] H. Kuramochi, T. Uzumaki, M. Yasutake, A. Tanaka, H. Akinage, and H. Yokoyama, Nanotechnology **16**, 24 (2005).
[2] S. J. Bending, Adv. Phys. **48**, 449 (1999).
[3] A. Sandhu, A. Okamoto, and I. Shibasaki, Microelectron. Eng. **73–74**, 524 (2004).
[4] J. Clarke and A. I. Braginski, *The SQUID Handbook* (Wiley, New York, 2006), Vol. 2, p. 408.
[5] X. Liu, D. Mazumdar, W. Shen, B. D. Schrag, and G. Xiao, Appl. Phys. Lett. **89**, 023504 (2006).
[6] S. Stein, M. Wuttig, D. Viehland, and E. Quandt, J. Appl. Phys. **97**, 1 (2005).
[7] S. Dong, J. Zhai, J. Bai, J. Li, and D. Viehland, Appl. Phys. Lett. **87**, 062502 (2005).
[8] S. Dong, J. Cheng, J. Li, and D. Viehland, Appl. Phys. Lett. **83**, 4812 (2003).
[9] J. Zhai, S. Dong, Z. Xing, J. Li, and D. Viehland, Appl. Phys. Lett. **89**, 083507 (2006).
[10] Z. Xing, S. Dong, J. Li, and D. Viehland, Appl. Phys. Lett. **88**, 062510 (2006).
[11] J. P. Teter, M. Wun-Fogle, A. E. Clark, and K. Mahoney, J. Appl. Phys. **67**, 5004 (1990).
[12] R. M. Bozorth, *Ferromagnetism* (Wiley, New York, 1993), p. 845.
[13] M. R. Sheinfein, J. Unguris, D. T. Pierce, and R. J. Celotta, J. Appl. Phys. **67**, 5932 (1990).
[14] T. Chang, M. Lagerquist, J.-G. Zhu, and J. H. Judy, IEEE Trans. Magn. **28**, 3138 (1992).